

Step fluctuation studies of surface diffusion and step stiffness for the Ni(111) surface

M. Ondrejcek,* M. Rajappan, W. Swiech, and C. P. Flynn

Department of Physics and Materials Research Laboratory, University of Illinois at Urbana-Champaign, Urbana, Illinois 61801, USA

(Received 16 August 2005; revised manuscript received 25 October 2005; published 12 January 2006)

Step edge fluctuations on clean Ni(111) are investigated using low-energy electron microscopy. When interpreted as capillary waves the fluctuations yield values of the surface mass diffusion coefficient D_s and the step edge stiffness $\tilde{\beta}$ in the temperature range 1050–1340 K. $\tilde{\beta}(\theta, T)$ is of magnitude ~ 300 meV/nm at 1200 K, almost independent of step orientation θ , and decreases with increasing temperature T . At the lower temperatures, the decay of capillary modes depends on wave vector q as q^3 , as expected for surface diffusion over terraces next to the step. Also, the deduced surface diffusion coefficient $D_s = 10^{-4 \pm 0.5} \exp \times (-0.65 \mp 0.1 \text{ eV}/k_B T) \text{ cm}^2/\text{s}$ is consistent with that on similar surfaces when scaled to homologous temperatures by the melting temperature T_m , in keeping with a recently suggested universality. A component of step relaxation driven by bulk diffusion above $0.65T_m$ is reasonably consistent with bulk diffusion results obtained much earlier using radio tracer methods. This result is contrasted with earlier discussions that postulate a regime of high-temperature surface diffusion with a large activation energy and very large prefactor. Sublimation detected here by step edge flow near $0.75T_m$ is consistent with the known cohesive energy.

DOI: [10.1103/PhysRevB.73.035418](https://doi.org/10.1103/PhysRevB.73.035418)

PACS number(s): 68.35.Fx, 68.37.Nq, 66.30.-h

I. INTRODUCTION

Diffusion on the surfaces of crystals has been studied for almost a century.¹ It is a central component in many processes of practical importance, such as the kinetics of chemical reactivity,² the stability of growth modes,³ and the physical smoothing that occurs on surfaces held at high temperatures.⁴ Seminal papers by Mullins⁵ distinguish surface diffusion from other processes, such as bulk diffusion, vapor transport, and plastic flow, that also contribute to smoothing, and establish that the several processes could be identified by their differing dependences on the particular wavelength representative of the roughness.

For clarity it is necessary to recognize two different diffusion coefficients. First, there is the hopping diffusion coefficient of surface atoms that measures the mean-square displacement of each mobile atom over a given time interval, as reviewed, for example, by Kellogg⁶ and by Ehrlich.⁷ Second, there is the mass diffusion coefficient that measures the surface flux of a species in response to a gradient of chemical potential, as reviewed by Seebauer and Allen⁸ and Bonzel.⁹ Reviews that focus on adsorbate diffusion are given by Gomer¹⁰ and by Naumovets and Vedula.¹¹ The surface mass diffusion coefficient D_s contains the equilibrium fraction of mobile atoms in addition to the hopping diffusion rate. It is the quantity of central interest in the present paper.

An extensive literature^{8,9} discusses two characteristic temperature regimes of diffusion that contribute to surface smoothing. First, at high temperatures, near the melting temperature T_m , D_s has a high activation energy comparable to that of the bulk, and a high prefactor $\sim 10^4 \text{ cm}^2/\text{s}$. Second, in a low-temperature regime $T < 0.6T_m$, D_s has a small activation energy and prefactor $\sim 10^{-4} \text{ cm}^2/\text{s}$. These possibilities are clarified in the present research. Specifically, it is shown here for Ni(111) that the high-temperature regime comprises volume diffusion misinterpreted as surface diffusion.

In this paper, we report measurements of surface mass diffusion on the clean (111) surface of fcc nickel. Low-index

Ni surfaces have been studied extensively in the past, by both experiment and theory, partly due to the technological importance of nickel and its compounds. Recent experiments^{12–14} deal mainly with Ni oxidation, Ni-based catalysis, and Ni alloys. Studies of diffusion, energetics, and morphology on clean Ni terraces remain important as models of more complex systems. Single and multiple steps formed on vicinal Ni(111) were observed in low-energy electron diffraction (LEED) research¹⁵ prompted by observed Ni(111) faceting at 1500 K.^{16,17} Single-adatom diffusion observed by field ion microscopy (FIM)¹⁸ appears to be the only diffusion study of nickel surfaces since Bonzel and Latta's¹⁹ 1978 report of D_s for Ni(110). Hopping and mass self-diffusion are summarized by Seebauer and Allen,⁸ and theoretical studies by Liu *et al.*²⁰ A brief summary follows.

Surface mass diffusion on Ni was studied during the period 1960–1980. Maiya and Blakely¹⁶ and Blakely and Mykura²¹ obtained $E_d = 0.62 \text{ eV}$ and $D_0 \sim 5 \times 10^{-4} \text{ cm}^2/\text{s}$ for vicinal Ni(111) from the observed relaxation of sinusoidal surfaces (etched “scratches”) at temperatures between 1075 and 1475 K ($0.6 < T < 0.85T_m$) using interferometry. They recognized Mullins' view⁵ that surface and bulk processes could be distinguished by their wavelength dependences, but used samples that faceted and were not well cleaned by today's standards. With scratches $\sim 10 \mu\text{m}$ wide and high-precision profilometry, Azzeri and Colombo¹⁷ obtained $D_0 \sim 10^5 \text{ cm}^2 \text{ s}^{-1}$ and $E_d = 2.79 \text{ eV}$ for $T > 0.75 T_m$ (1300 K), and confirmed that Ni(111) facets at 1500 K. In other reports, E_d varied from 0.82 at low T and for cleaner surfaces, to 1.85 eV for low-index surface planes studied by interferometry^{16,22} for $T > 0.6 T_m$ or field emission microscopy (FEM) at lower T .^{23,24} The prefactors D_0 ranged from 0.01 to tens of $\text{cm}^2 \text{ s}^{-1}$ for $T < 0.45 T_m$ (see Ref. 8). The FEM technique averages diffusion processes over a range of surface planes; E_d rose from 1.08 eV on clean Ni to 1.17 eV with 0.3 ML sulfur.²⁴ Bonzel and Latta¹⁹ used interference methods on Ni(011) in UHV to find two

temperature regimes. Below 1150 K with $D_s=9\times 10^{-3}\exp(-0.76\text{ eV}/k_B T)\text{ cm}^2/\text{s}$ along $[1\bar{1}0]$ and $D_s=470\times\exp(-1.95\text{ eV}/k_B T)\text{ cm}^2/\text{s}$ along $[001]$. Above 1150 K, the diffusion was isotropic and similar to the latter values. The wavelength dependence was omitted as a means to identify mechanisms, and a variety of explanations were proposed for different observed regimes.^{25,8,19}

Hopping diffusion of single atoms has been examined by FIM at low T . The activation energy of adatoms on Ni(111) is 0.33 eV (Ref. 26) or 0.22 eV (Ref. 18) with a prefactor $\sim 10^{-5}\text{ cm}^2/\text{s}$. $E_d=0.84\text{ eV}$ for step edge atoms ascending to the upper terrace (which includes adatom formation).

Only over the past few years has the role of bulk diffusion in surface processes, identified by Blakely and Mykura²⁷ for scratch smoothing, been quantified more precisely for Pt(111) and Pd(111).^{28,29} The two contributions to step relaxation of (i) bulk vacancy flow and (ii) surface defect flow over terraces, exchange dominance from the former to the latter as the temperature is lowered through about $0.65T_m$. Surfaces as sources for bulk defects have been documented for Pt(111) (Ref. 30) and NiAl(011).³¹

In a number of recent publications,^{28,29,32-34} we discuss step fluctuation spectroscopy as a means to explore the energetics of straight steps and the diffusive relaxation of step profiles on the clean, close-packed surfaces of vacuum-compatible metals. The analysis makes use of step profiles recorded as video sequences obtained by low-energy electron microscopy (LEEM). Earlier work examined the behavior on Si(100) (Ref. 35) and Si(111).³⁶ One main merit of the approach is that step fluctuations, interpreted as capillary waves, offer explicit signatures that confirm the assumed capillary character of the process. Thus, the step stiffness $\tilde{\beta}(\theta, T)$, for the given temperature T and step orientation θ , follows directly³⁷ from equipartition as

$$\langle |y_q|^2 \rangle = \frac{k_B T}{\tilde{\beta} q^2 L}. \quad (1)$$

Reviews of step behavior are available.^{38,39} Similar formula describes amplitudes in real space rather than Fourier space.⁴⁰ In Eq. (1), y_q is the wave amplitude (Fourier component q of the step profile) and L the length of step analyzed; the step stiffness $\tilde{\beta}$ is related to the free energy per unit length (line tension) β by

$$\tilde{\beta} = \beta + \frac{\partial^2 \beta}{\partial \theta^2} \quad (2)$$

The important point is that the dependence of Eq. (1) on wave vector as q^{-2} can be checked experimentally to verify the assumed capillary behavior.

In a similar way, the kinetics of the step profile fluctuations offer explicit signatures that help to identify particular operative mechanisms. Step fluctuations relax because fluxes of thermal defects respond to the chemical potential difference between points of negative and positive step curvature, owing to the Gibbs-Thompson effect; this flow transports

matter that reduces the amplitude of the fluctuation. Fourier amplitudes relax exponentially with rates determined from correlation measurements. Thus,

$$\langle y_q(t') y_q^*(t) \rangle = \langle |y_q(t)|^2 \rangle \exp\left[\frac{-(t' - t)}{\tau_q} \right], \quad (t' > t) \quad (3)$$

where, for relaxation by surface diffusion,^{34,38}

$$\tau_q^{-1} = \frac{2A\tilde{\beta}D_s q^3}{k_B T} \quad (4)$$

and for relaxation by bulk diffusion,²⁸

$$\tau_q^{-1} = \frac{\pi A \tilde{\beta} D_b q^2}{a k_B T} \quad (5)$$

In these equations, D_s and D_b are the surface and bulk mass diffusion coefficients, A is the surface area per atom, and a is the interplanar spacing. Experiments that explore step fluctuations can employ the different explicit q dependences to identify the two different mechanisms in practical cases. In the recent experiments, these factors are employed to distinguish surface diffusion from bulk diffusion. When two mechanisms occur together, it is commonly assumed that their effects are additive so that

$$\tau_q^{-1} = \pi \left(D_b + \frac{2qa}{\pi} D_s \right) \frac{A\tilde{\beta}q^2}{a k_B T} \quad (6)$$

although this is not proven. Behavior in crossover regimes has been discussed explicitly.⁴¹⁻⁴³ It bears comment that neither $\tilde{\beta}(\theta, T)$ nor D_s has proved easy to measure by alternative methods. Bulk diffusion is known from radio tracer measurements.⁴⁴⁻⁴⁶

The research reported in the present paper continues an effort to investigate the surface properties of vacuum-compatible metals at elevated temperatures. Here we report step fluctuation results for Ni(111). In combination with earlier results for Pd(111) and Pt(111), the Ni(111) results complete examination of a column of similar metals from the periodic table and, thus, affords interesting comparisons. Our discussion of Ni diffusion differs from earlier treatment. We show that behavior at high temperatures can be explained by dominant bulk diffusion rather than by surface diffusion and that the large activation energy and very large prefactor then have natural explanations. Sublimation detected here by step flow observed near $0.75T_m$ is consistent with the known cohesive energy.

Section II of the paper summarizes experimental details. Section III reports our results for Ni(111), and Sec. IV discusses matters of further interest.

II. EXPERIMENTAL

As details of the equipment and analysis procedures have been presented in earlier publications,^{29,32} only a brief summary is needed here. A LEEM designed and built by Tromp⁴⁷ has been modified with *in situ* sample preparation and processing capabilities; it has a base pressure in the 10^{-11} torr

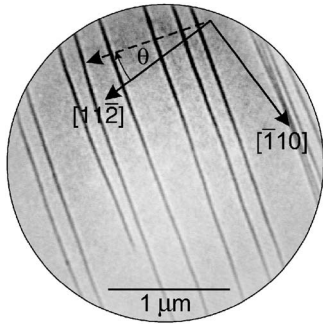


FIG. 1. LEEM image showing nearly ideal straight step edges on the Ni(111) surface at 1150 K (impact energy $E=4$ eV). The broken arrow indicates the average step orientation (normal to the step length) of $\theta=-18^\circ$ relative to the close-packed direction (obtained from a LEED image not shown). The steps pass uphill from left to right. A screw dislocation occurs where the step terminates (lower left).

range and operates with samples up to 1700 K.

A single crystal of Ni(111) 9 mm diameter, with the front surface miscut by $\sim 0.2^\circ$, was purchased from the Surface Preparation Laboratory. Two independent series of experiments were performed, each preceded by a full cleaning procedure as follows. The initial cleaning, in a UHV preparation chamber with LEED optics, used cycles of 1 keV Ar^+ ion bombardment at room temperature followed by annealing in UHV at 1050 K, and occasionally in 10^{-6} Pa of O_2 . The crystal was also heated for several days in 5×10^{-5} Pa of H_2 to remove bulk sulfur, until it attained a $p(1 \times 1)$ LEED pattern with sharp spots. After a final heating close to the maximum experimental temperature of 1350 K, the crystal was quickly transferred under N_2 to the LEEM introduction stage, and Ar^+ , O_2 , and H_2 cleaning resumed for several days, with Auger electron spectroscopy (AES), LEED, and LEEM employed to monitor surface conditions. Auger analysis revealed a trace of new surface sulfur after an extended anneal at high temperature, but the clean surface could be restored by fresh sputtering followed by a modest anneal. A typical LEEM image of the clean surface with almost parallel steps is given in Fig. 1.

Video sequences from the cleaned crystal were rotated, digitized, and Fourier amplitudes of step profile $y_q(t)$ determined frame by frame, so that mean-square amplitudes $\langle |y_q(t)|^2 \rangle$ and correlation functions $\langle y_q(t') y_q^*(t) \rangle$ could be extracted for each sequence. Methods described elsewhere correct these results for spatial and temporal resolution, pixel noise, and nonzero correlations at long times arising from bent or tilted steps.²⁹ These procedures yield amplitudes to ~ 1 nm for wavelengths $2\pi/q > 100$ nm, and relaxation times $\tau_q > 30$ ms.

The q^{-2} variation of $\langle |y_q(t)|^2 \rangle$ expected for capillary waves was generally observed, as illustrated in Fig. 2 for a step studied at 1105 K. Each individual q then defines a value of $\tilde{\beta}$ as shown in inset in Fig. 2(b), from which a best mean can be selected. These provided the final data for step stiffness at any given temperature. Correlation functions were fitted to exponential decays, as in the example for $T=1105$ K shown in Fig. 3(a). It will be apparent in some cases that the func-

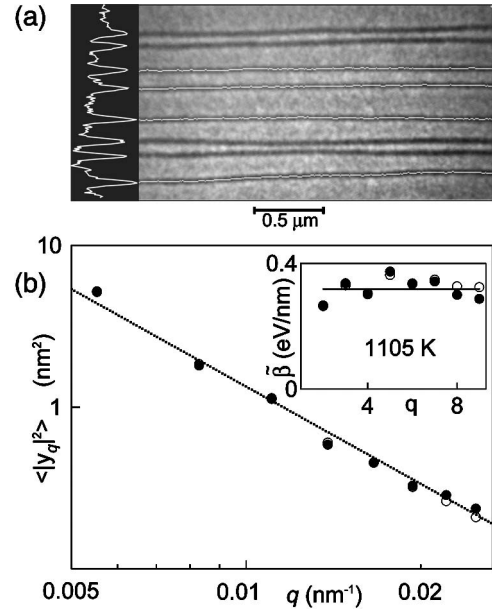


FIG. 2. (a) Steps marked by fitting Gaussians to the intensity profiles (1105 K, $E=4$ eV). (b) Squared Fourier amplitudes at 1105 K shown as a function of q for a single Ni step. Open circles are raw data and full points are corrected for constant pixel noise, spatial, and temporal resolutions. A straight line fit shows the q^{-2} dependence of amplitudes expected for capillary waves. Inset shows the variations of deduced stiffness with q . 1 frame (1f)=1/30 s, $q[\text{nm}^{-1}]=2\pi q/L$, $q=1, 2, \dots$, integral and $L \sim 2.2 \mu\text{m}$.

tion fails to reach zero at long times, for which the correction mentioned above becomes necessary.³² The resulting relaxation times exemplified in Fig. 3(b) were employed, as described in Sec. III, to determine diffusive properties and, in particular, to separate the surface and bulk contributions to the observed step relaxation.

The lowest temperatures for data acquisition in the present research were set by the expanding time scale, which generally exceeded the experimental constraints of image drift and microscope stage stability at temperatures below about $T_m/2$. The upper temperature limit was set by sample evaporation, generally visible as a steady drift of the step edges progressively across the screen, at speeds that increase with T . A few runs were taken in this regime, with results described below in Sec. III. Also, at these temperatures, fewer than six modes were accessible because relaxation rates for larger q exceeded the available time resolution (1 frame=33 ms).

III. RESULTS

Here we present results for (i) step stiffnesses and energies, including the relationship to island shapes; (ii) surface and bulk diffusion; and (iii) sublimation of Ni(111) at high temperatures.

A. Step stiffness on Ni(111)

Ni melts at $T_m=1728$ K. Step stiffness measurements were completed in this research through the temperature

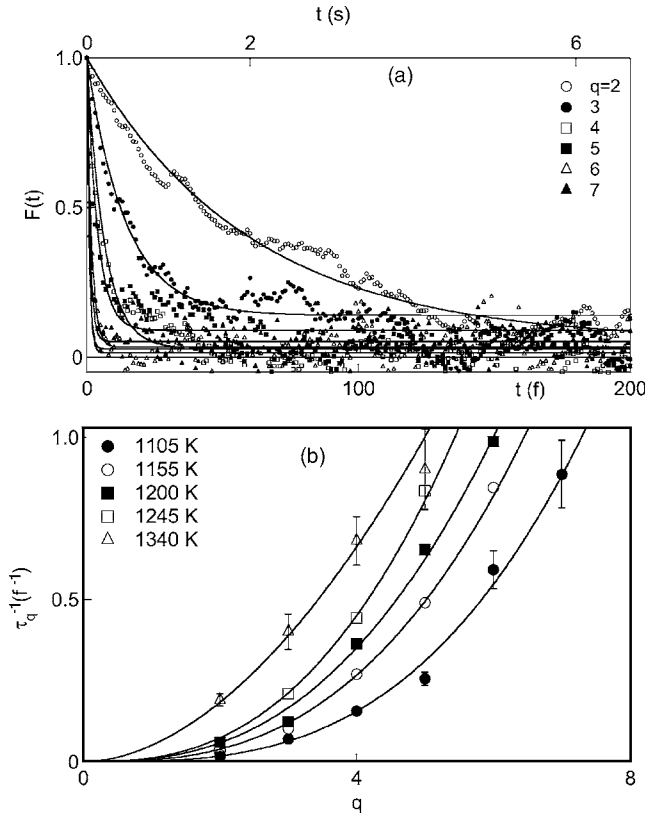


FIG. 3. (a) Exponential fits to time correlations $F(t)$ for several q at 1105 K obtained with Hanning window function to suppress end effects. (b) Power-law fits q^α to relaxation rates for five temperatures $\alpha=3.1\pm 0.1$ at 1105 K, 2.8 ± 0.1 at 1155 K, 2.6 ± 0.2 at 1200 K, 2.6 ± 0.1 at 1245 K, and 1.9 ± 0.1 at 1340 K. The results are near q^3 at low temperature as predicted for terrace diffusion. No sharp transition to q^2 occurs at higher T . Values above $T \sim 1280$ K are influenced by sublimation.

range $0.5T_m < T < 0.67T_m$ or $1050 \text{ K} < T < 1340 \text{ K}$. Values of $\bar{\beta}$ thus obtained are shown as a function of T in Fig. 4(a). The variation is featureless within experimental uncertainty, and with a decreasing trend with temperature increase. The broken line represents a least-squares fit to the unweighted experimental points.

Various areas of the annealed crystal possessed slightly differing miscuts. This made possible studies of the step properties as a function of step orientation relative to the surface crystallographic axes. Ni(111) has 3 m symmetry so at least 60° of data are needed to fully fix the angular behavior. A total of 50 lines were studied for 13 angles in the range $-28^\circ < \theta < 75^\circ$. Results are presented in Fig. 4(b) as a plot of $\bar{\beta}(\theta)/\bar{\beta}$ at 1155 K, with $\bar{\beta}$ the angular average. By deriving the relative stiffnesses from fits to the q dependence of the Hanning relaxation rates, using Eq. (4), we avoided added scatter from the triangle subtraction analysis.²⁹ The advantage of this choice is certainly evident in the data of Fig. 4(b); also, little or no dependence of $\bar{\beta}$ on θ is visible. In connection with this latter observation, we have also studied the shapes of islands occasionally present on otherwise featureless terraces. The islands are notably isotropic, as may be seen, for example, in Fig. 4(c). It is known that the island

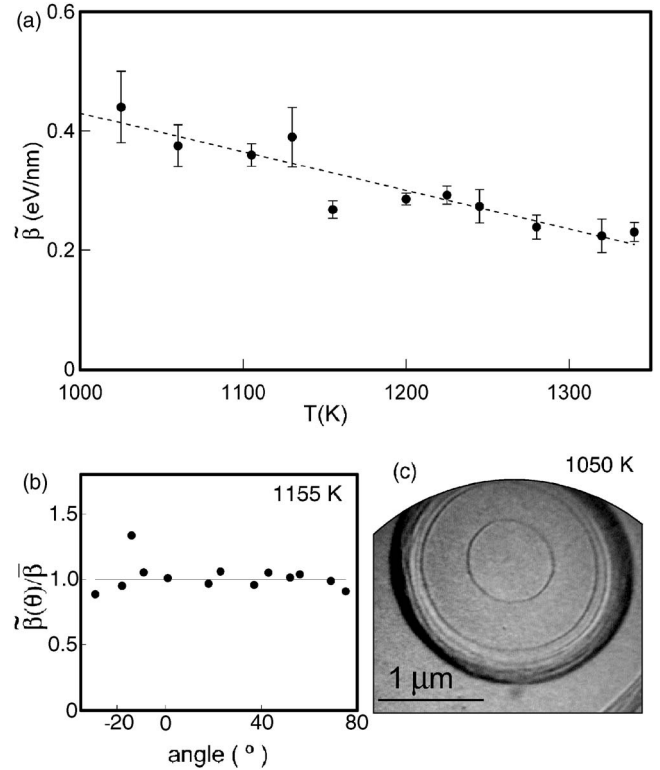


FIG. 4. (a) Average step stiffness on Ni(111) shown as a function of temperature. The line is a least-squares fit. (b) Angle dependence of stiffness derived from relaxation rates (see text). Stiffness exhibits little or no dependence on step orientation. (c) Observed island shape measured at 1050 K confirms the almost isotropic step free energy.

shape is related to the step free energy β through a Wulff transformation,⁴⁸ with β , in turn, related to $\bar{\beta}$ through the Legendre transformation, Eq. (2). The circular island shape thus provides a sensitive confirmation of the isotropy of $\bar{\beta}$ determined here from step fluctuations [see Fig. 4(b)].

B. Surface and bulk diffusion

It is not initially known whether the observed step relaxation at these temperatures is due to the motion of atoms by surface or by bulk diffusion. A means to distinguish between these processes is provided by their dependence on fluctuation wave vector q , as detailed above. With the surface contribution to τ_q^{-1} varying as q^3 and the bulk as q^2 , the two may be separated by a method that is described by Ondrejcek *et al.*,²⁹ with $(\tau_q q^2)^{-1}$ shown as a function of q . Then, the intercept at $q=0$ gives the contribution of bulk diffusion and the slope reflects the surface diffusion alone. Implicit in this treatment²⁸ is the assumption that surface and bulk effects are simply additive in the net relaxation [Eq. (6)], although this remains still to be demonstrated for practical examples.

Figure 5 illustrates the results for the case of Ni(111). Straight lines of non-negative intercept are first fitted to the data for the lowest temperatures. Their slopes indicate surface diffusion coefficients shown in Fig. 6(a). Intercepts are plotted in Fig. 6(b) as values of the bulk diffusion coefficient.

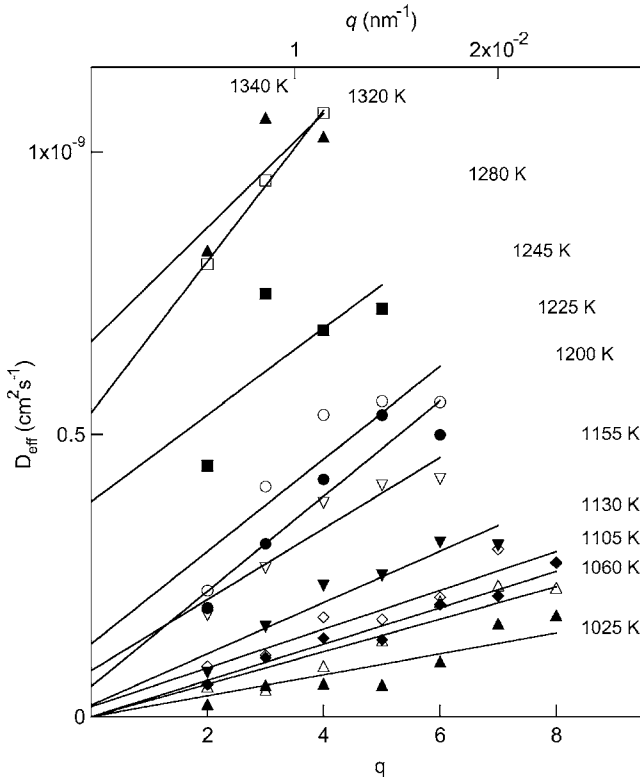


FIG. 5. Effective diffusion coefficients for Ni(111) at various temperatures plotted as a function of wave number q from Eqs. (4) and (5). From Eq. (6), the slope fixes the D_s at any given T and the intercept gives D_b .

The surface diffusion determined in this way is

$$D_s(T) = 10^{-4 \pm 0.5} \exp(-0.65 \mp 0.1 \text{ eV}/k_B T) \text{ cm}^2/\text{s}$$

(a least-squares fit gave an actual prefactor $9.3 \times 10^{-5} \text{ cm}^2/\text{s}$). Further comments on this result are deferred to Sec. IV.

The data for bulk diffusion obtained here do define a magnitude of diffusion but are not precise enough to offer an independent assessment of an activation energy and prefactor. Shown as a broken line in Fig. 6(b) is the bulk diffusion predicted from diffusion parameters determined earlier by radio tracer measurements.^{46,49} These are smaller than the present values by an order of magnitude. It is worth noting in this connection that tracer measurements are confined to temperatures much higher than those employed here; thus, the results shown derive from measurements closer to T_m . A tendency for Arrhenius plots for bulk diffusion to curve to higher values at lower temperatures^{44,45} has been widely recognized, and this is reasonably consistent with Fig. 6(b).

A final important point in this same connection is presented in Fig. 7(a), which shows a surface diffusion as a function of reciprocal temperature determined by assuming that the relaxation times are attributable to surface diffusion throughout the entire range (they are instead due to bulk diffusion in the upper part of the range). The dotted line at low temperatures in the figure correspond to surface diffusion, and the broken line at high temperature indicates a

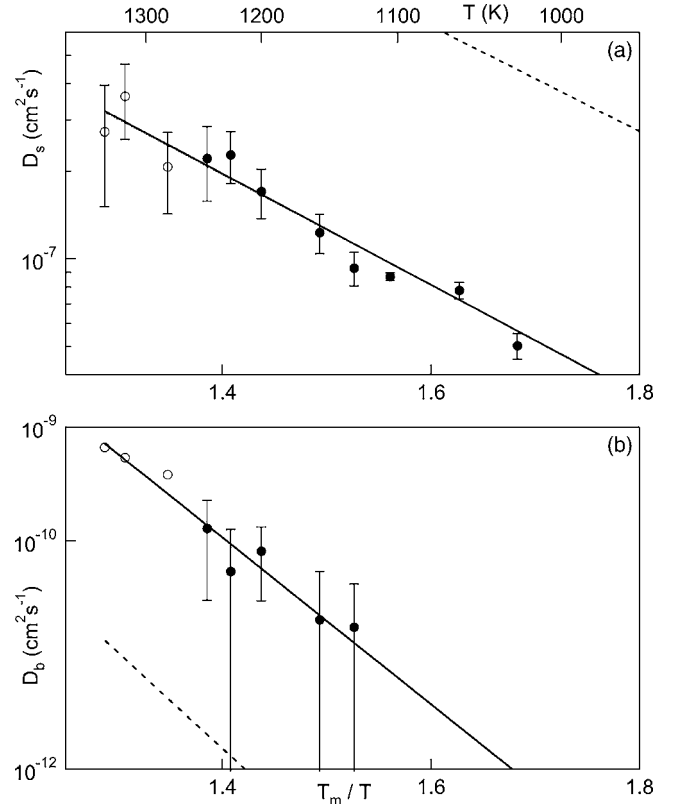


FIG. 6. Surface (a) and bulk (b) diffusion coefficients for Ni(111) obtained by fits to Fig. 5. The scatter is large in (a) at high T and in (b) at low T , owing to dominance of the competing process. In (a) the solid line is a least-squares fit with $D_s = 9.3 \times 10^{-5} \exp(-0.65 \text{ eV}/k_B T) \text{ cm}^2/\text{s}$. The dashed line shows result of earlier surface smoothing with $D_s = 5 \times 10^{-4} \exp(-0.62 \text{ eV}/k_B T) \text{ cm}^2/\text{s}$. In (b) the fit for high T (solid line) is $D_b \sim 1.4 \exp(-2.49 \text{ eV}/k_B T) \text{ cm}^2/\text{s}$ and the dashed line is $D_b = 0.92 \exp(-2.88 \text{ eV}/k_B T) \text{ cm}^2/\text{s}$ from radio tracer results. Open circles mark data obtained in the step flow regime in which Ni sublimates.

fictitious surface diffusion with an activation energy that corresponds to bulk diffusion. We return in Sec. IV to the way this behavior illuminates the mistaken earlier speculations^{8,9} about high- and low-temperature domains of surface diffusion.

C. Sublimation of Ni(111)

An uphill advance of steps over time is observed in a temperature range above 1260 K where sublimation is expected.¹⁹ For step velocities of $\sim 1 \text{ nm/s}$, the process is slower than that associated with most step fluctuations and is therefore expected to take place with the surface-defect system very close to equilibrium. This entails provision by steps of equilibrium proportions of adatoms to the terraces, with an activation energy of the adatom formation free energy E_a , followed by evaporation of adatoms from the terraces with the required activation energy of the cohesive energy $E_c - E_a$. The net activation energy for the process at equilibrium is therefore $E_c = 4.45 \text{ eV}$ for Ni.⁵⁰ In principle, this value re-

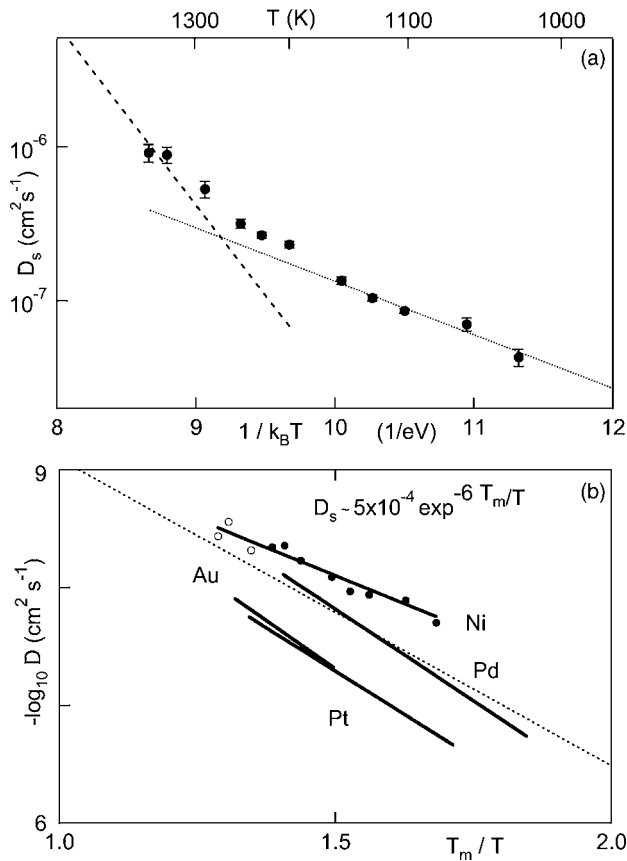


FIG. 7. (a) Variation with T of effective D_s for Ni(111) surface diffusion with coefficients evaluated from the relaxation times [Eq. (4)]. At low T , data points are similar to Fig. 6(a) and dotted line is $D_s = 4 \times 10^{-4} \exp(-0.8 \text{ eV}/k_B T) \text{ cm}^2/\text{s}$. At high T , the broken line is $D_s = 1.5 \times 10^{-4} \exp(-2.7 \text{ eV}/k_B T) \text{ cm}^2/\text{s}$ with the bulk activation energy (the actual process is *not* surface diffusion). (b) Surface mass diffusion for close packed fcc surfaces Pt, Pd, Au, and Ni, shown as functions of T_m/T . The values are similar to an earlier suggestion of universal $D_s \sim 10^{-4} \exp(-6 T_m/T) \text{ cm}^2/\text{s}$ indicated by the broken line.

quires correction for thermal contributions to the free energy difference with the vapor phase, which, however, amount only to tenths of electron volts per atom and which fall below the precision available to the present observations.

Figure 8(a) presents images of steps on Ni(111) taken during sublimation, which causes steps to flow “uphill” as time progresses. In this figure, steps flow about $0.5 \mu\text{m}$ (arrow) in 45 s. The step flow is quantified by a screw dislocation, made easily visible in the images, by the termination of the surface step at the point where the screw intersects the surface. The process in which a screw passes through a step is itself of interest. It is discussed elsewhere⁵¹ for the case of Nb(011). Here we employ the screw dislocation, presumed immobile relative to the Ni lattice, as a fiducial marker to fix the locations of neighboring step edges as functions of time in a way that eliminates temporal drifts of the microscope stage. In Fig. 8(b) are shown, for the three temperatures studied here, the neighboring step positions in successive video frames, relative to the screw dislocation. These positions define mean velocities that are shown as functions of reciprocal

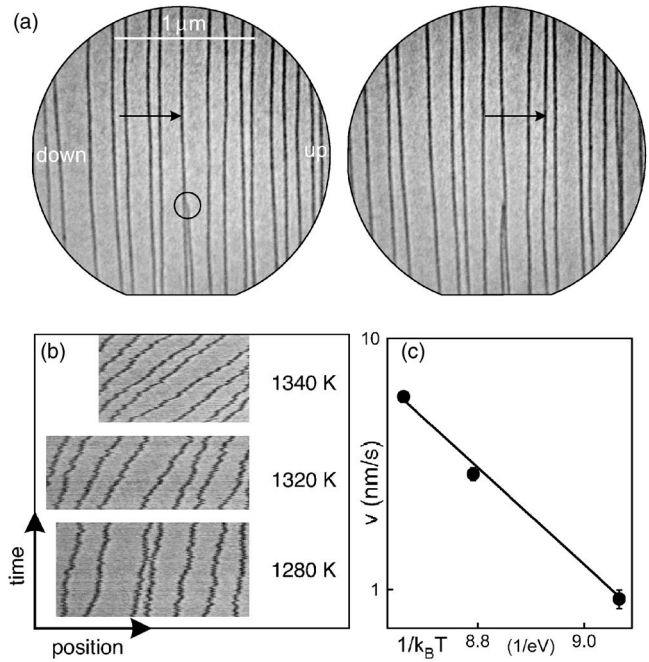


FIG. 8. (a) Uphill step flow from sublimation at 1340 K is visible in LEEM images taken 45 s apart (arrows). A stationary screw dislocation serves as the fiducial point for the time series. (b) Time dependence of step positions relative to screw at 1280, 1320, and 1340 K. (c) Arrhenius plot of average velocities from (b) and slope fitted well with Ni cohesive energy of 4.45 eV (solid line).

temperature in Fig. 8(b). The line drawn through the points represents an activation energy of 4.45 eV equal to the cohesive energy. A least-squares fit yields instead 4.7 eV. The precision of the measurements does not warrant inferences drawn from these small differences. However, it is possible to conclude that the sublimation process is, indeed, sufficiently slow that the surface defect system remains close to the equilibrium configuration. Similar conclusions have been drawn from reflection electron microscopy observations on evaporating Si(111).⁵²

IV. DISCUSSION

Here we offer further comments that place the measured step stiffnesses and measured surface diffusion coefficients in a larger context.

With regard to the step stiffness we note that the present results for Ni(111) complete investigations of a column of similar metals in the periodic table begun by work²⁹ on Pd(111) and Pt(111). Some review of overall behavior is therefore possible. At $\sim 300 \text{ meV}/\text{nm}$ the step stiffness of Ni(111) is a little larger than that of the heavier metals. In all three cases, the stiffness is temperature dependent, with that for Ni decreasing most rapidly with T . In no case is there any evidence for a step-roughening transition associated with a vanishing step free energy, even though the measurements approach 70% of the melting temperature. Surface roughening has been reported for Ni(011) above 1300 K.⁵³

A second matter of interest is the anisotropy of the step stiffness. All three metals have relatively isotropic stiffnesses

and, consequently, step free energies that are still more isotropic by a factor of at least $3^2 - 1 = 8$, where 3 recognizes the 3m symmetry of the fcc (111) surface.^{32,33} Of the three metals, Ni is the most isotropic, with little or no observed angular dependence of island shape or step fluctuations in the present temperature range. The sixfold anisotropy on Pd(111) is 25% between $\langle 11\bar{2} \rangle$ and $\langle \bar{1}10 \rangle$, the former being the larger, and is 10% for Pt(111). It is notable here that the anisotropy does not correlate smoothly with atomic mass. In other work it is found that Au(111)³³ and Mo(011)³² exhibit very large anisotropies of step stiffness. Apparently, no predictive theory is as yet available to explain these important characteristics.

Turning now to the observed surface diffusion, the results invite comparison on a still broader scale. Evidence has recently been put forward that surface mass diffusion on the close-packed surfaces of vacuum compatible metals conforms to an unexpected type of universality.^{54,55,29} The behavior is similar to that, long recognized but still unexplained, for bulk diffusion, which follows the relationship $D_b = 0.3 \exp(-17T_m/T) \text{ cm}^2/\text{s}$ with fair accuracy.^{43,44} Thus all metals have approximately the same mass diffusion when temperatures are scaled to T_m . A similarly homologous behavior has recently been attributed to surface mass diffusion,^{55,29} as mentioned above.

To see how the Ni(111) results fit into these observations, Fig. 7(b) shows the surface diffusion on Ni(111), Pt(111), Pd(111), and Au(111) as functions of T_m/T . The results do, indeed, lie generally within a factor 3 of average values, suggested earlier⁵⁵ to be $D_s = 5 \times 10^{-4} \exp(-6T_m/T) \text{ cm}^2/\text{s}$, and indicated by the broken line in the figure. Further work is, of course, needed to determine the degree to which all (111) metal surfaces conform to the trend and whether other surfaces behave the same way. Any explanation of such universality requires⁵⁶ that the ratio of two specific integrals over the configuration spaces of the crystal must take a particular value. No reason why this must be the case has, as yet, been identified.

We return finally to the topic of high- and low-temperature regimes of surface diffusion on metal surfaces that remains unresolved in the literature of this area, as reviewed in Sec. I. The matter in question originates in the study of surface smoothing (scratch annealing), in which Mullins predicts a q^4 dependence for two-dimensional surfaces with relaxation driven by surface diffusion, and a q^3 dependence for relaxation by diffusion through the bulk (i.e., by bulk vacancies). This differs from the behavior in the present study of one-dimensional step edges where the surface diffusion drives step relaxation with kinetics dependent on q^3 , while the bulk process gives q^2 (with logarithmic corrections). In the present study, the q dependence is employed

to separate the physical mechanisms, as in the use by Blakely and Mykura²⁷ of Mullins' predictions.⁵ Our analysis thus provides an unambiguous assignment of processes at $T < 0.65 T_m$ to surface diffusion, and those at higher temperatures to step relaxation driven by bulk vacancy diffusion.

It is suggestive, by analogy, that the earlier anomalous results for surface smoothing, described in the Introduction, derive from surface diffusion at low temperatures, but from bulk diffusion rather than the presumed surface diffusion at high temperatures. This overview, nevertheless, remains to be demonstrated as a fact. One key to this recognition derives from Fig. 7(a). In the upper temperature range of step relaxation, where bulk diffusion becomes dominant, the effective surface diffusion coefficient shown there has an unrealistic prefactor $D_0 \sim 10^4 \text{ cm}^2/\text{s}$, suggestive of long jumps or other conceived physical processes. This perspective is, however, entirely spurious. In fact, the large prefactor results from the incorrect ascription of a bulk process to surface diffusion.

The final point to be made here is that this is a more general problem, not directly dependent on the question of whether step relaxation or surface smoothing is the matter under discussion. To see this, suppose generally that two processes $D_1 \exp(-Q_1/k_B T)$ and $D_2 \exp(-Q_2/k_B T)$ compete in contributing additively to any particular observed quantity, such that their contributions cross at $T = \alpha T_m$. Then,

$$D_1 = D_2 \exp[-(Q_1 - Q_2) / \alpha k_B T_m].$$

For the phenomena of concern here $Q_1 - Q_2 \sim 1 \text{ eV}$ while $k_B T_m \sim 0.1 \text{ eV}$, and $\alpha \sim 2/3$ since the crossover occurs near $0.65 T_m$. It follows that prefactors must be in the ratio $D_1/D_2 \sim e^{15} \sim 3 \times 10^6$. This is the correct order of magnitude to explain reported prefactors for "surface diffusion" in the high-temperature regime,^{8,19} which are a factor $\sim 10^6$ larger than the prefactors $\sim 10^{-3} \text{ cm}^2/\text{s}$ that are reported for actual surface diffusion at lower temperatures. Thus the early and confused data for surface diffusion are consistent with the present results from step fluctuations, and with the related conclusion that bulk diffusion prevails over surface diffusion in surface smoothing at high temperatures. It appears that this conclusion could have been evident beforehand had the identification of specific mechanisms by their signature dependence on wave vector q been carried out also in the earlier research.

ACKNOWLEDGMENT

This research was supported in part by the Department of Energy Grant No. DEFG02-91ER45439, which includes the Center for Microanalysis of Materials in which the LEEM is maintained.

- *Corresponding author. Mailing address: Department of Physics, University of Illinois at Urbana-Champaign, 1110 W. Green Street, Urbana, Illinois 61801, USA. Email address: ondrejcek@uiuc.edu
- ¹G. Antczak and G. Ehrlich, *Surf. Sci.* **589**, 52 (2005).
 - ²R. Imbühl and G. Ertl, *Chem. Rev. (Washington, D.C.)* **95**, 697 (1995).
 - ³P. Politi, G. Grenet, A. Marty, A. Ponchet, and J. Villain, *Phys. Rep.* **324**, 271 (2000).
 - ⁴H. P. Bonzel and W. W. Mullins, *Surf. Sci.* **350**, 285 (1996); R. Panat, K. J. Hsia, and D. G. Cahill, *J. Appl. Phys.* **97**, 013521 (2005).
 - ⁵W. W. Mullins, *J. Appl. Phys.* **30**, 77 (1959).
 - ⁶G. L. Kellogg, *Surf. Sci. Rep.* **21**, 1 (1994).
 - ⁷G. Ehrlich, in *Surface Diffusion: Atomistic and Collective Processes*, edited by M. Tringides (Plenum, New York, 1997).
 - ⁸E. G. Seebauer and C. E. Allen, *Prog. Surf. Sci.* **49**, 265 (1995).
 - ⁹H. P. Bonzel, in *Diffusion in Solid Metals and Alloys*, edited by H. Mehrer, Landolt-Börnstein, New Series, Group III, Vol. 26 (Springer, Berlin, 1990), p. 717.
 - ¹⁰R. Gomer, *Rep. Prog. Phys.* **53**, 917 (1990).
 - ¹¹A. G. Naumovets and Y. S. Vedula, *Surf. Sci. Rep.* **4**, 365 (1985).
 - ¹²I. L. Bolotin, A. Kutana, B. Makarenko, and J. W. Rabalais, *Surf. Sci.* **472**, 205 (2001).
 - ¹³F. Zaera, *Prog. Surf. Sci.* **69**, 1 (2001); M. Ackermann, O. Robach, C. Walker, C. Quiros, H. Isern, and S. Ferrer, *Surf. Sci.* **557**, 21 (2004).
 - ¹⁴V. Shutthanandan, A. A. Saleh, and R. J. Smith, *Surf. Sci.* **450**, 204 (2000).
 - ¹⁵J. P. Chang and J. M. Blakely, *J. Vac. Sci. Technol. A* **10**, 2154 (1992).
 - ¹⁶P. S. Maiya and J. M. Blakely, *J. Appl. Phys.* **38**, 698 (1967).
 - ¹⁷N. Azzzeri and R. L. Colombo, *Metallography* **9**, 233 (1976).
 - ¹⁸T. Y. Fu and T. T. Tsong, *Surf. Sci.* **454-456**, 571 (2000).
 - ¹⁹H. P. Bonzel and E. E. Latta, *Surf. Sci.* **76**, 275 (1978).
 - ²⁰C. L. Liu, J. M. Cohen, J. B. Adams, and A. F. Voter, *Surf. Sci.* **253**, 334 (1991).
 - ²¹J. M. Blakely and H. Mykura, *Acta Metall.* **9**, 23 (1961).
 - ²²H. P. Bonzel and N. A. Gjostein, *J. Appl. Phys.* **39**, 3480 (1968).
 - ²³A. J. Melmed, *J. Appl. Phys.* **38**, 1885 (1967).
 - ²⁴M. Blaszczyzyn, *Surf. Sci.* **136**, 103 (1984).
 - ²⁵N. A. Gjostein, in *Surfaces and Interfaces I, Chemical and Physical Characteristics*, edited by J. J. Burke, N. L. Reed, and V. Weiss (Syracuse University Press, Syracuse 1967), p. 271.
 - ²⁶R. T. Tung and W. R. Graham, *Surf. Sci.* **97**, 73 (1980).
 - ²⁷J. M. Blakely and H. Mykura, *Acta Metall.* **10**, 565 (1962).
 - ²⁸M. Ondrejcek, W. Swiech, G. Yang, and C. P. Flynn, *Philos. Mag. Lett.* **84**, 69 (2004); **84**, 417 (2004).
 - ²⁹M. Ondrejcek, W. Swiech, M. Rajappan, and C. P. Flynn, *Phys. Rev. B* **72**, 085422 (2005).
 - ³⁰B. Poelsema, J. B. Hannon, N. C. Bartelt, and G. L. Kellogg, *Appl. Phys. Lett.* **84**, 2551 (2004).
 - ³¹K. F. McCarty, J. A. Nobel, and N. C. Bartelt, *Nature (London)* **412** 622 (2001); *Phys. Rev. B* **71**, 085421 (2005).
 - ³²M. Ondrejcek, W. Swiech, C. S. Durfee, and C. P. Flynn, *Surf. Sci.* **541**, 31 (2003).
 - ³³M. Ondrejcek, M. Rajappan, W. Swiech, and C. P. Flynn, *Surf. Sci.* **574**, 111 (2005).
 - ³⁴C. P. Flynn, *Phys. Rev. B* **66**, 155405 (2002).
 - ³⁵N. C. Bartelt, J. L. Goldberg, T. L. Einstein, E. D. Williams., J. C. Heyraud, and J. J. Metois, *Phys. Rev. B* **48**, 15453 (1993).
 - ³⁶N. C. Bartelt, R. M. Tromp, and E. D. Williams, *Phys. Rev. Lett.* **73**, 1656 (1994); N. C. Bartelt and R. M. Tromp, *Phys. Rev. B* **54**, 11 731 (1996).
 - ³⁷P. Nozières, in *Solids Far From Equilibrium*, edited by C. Godrèche (Cambridge University Press, Cambridge, England, 1991), p. 1.
 - ³⁸H.-C. Jeong and E. D. Williams, *Surf. Sci. Rep.* **34**, 171 (1999).
 - ³⁹M. Giesen, *Prog. Surf. Sci.* **68**, 1 (2001).
 - ⁴⁰O. Bondarchuk, D. B. Dougherty, M. Degawa, E. D. Williams, M. Constantin, C. Dasgupta, and S. Das Sarma, *Phys. Rev. B* **71**, 045426 (2005).
 - ⁴¹T. Ihle, C. Misbah, and O. Pierre-Louis, *Phys. Rev. B* **58**, 2289 (1998).
 - ⁴²S. V. Khare and T. L. Einstein, *Phys. Rev. B* **57**, 4782 (1998).
 - ⁴³B. Blagojevic and P. M. Duxbury, *Phys. Rev. E* **60**, 1279 (1999).
 - ⁴⁴N. L. Peterson, in *Solid State Physics*, edited by F. Seitz, D. Turnbull, and H. Ehrenreich (Academic Press, New York, 1968), Vol. 22, p. 409.
 - ⁴⁵C. P. Flynn, *Point Defects and Diffusion* (Oxford University Press, London, 1972).
 - ⁴⁶N. L. Peterson, *J. Nucl. Mater.* **69-70**, 3 (1978).
 - ⁴⁷R. M. Tromp and M. C. Reuter, *Ultramicroscopy* **36**, 99 (1991).
 - ⁴⁸A. Pimpinelli and J. Villain, *Physics of Crystal Growth* (Cambridge University Press, Cambridge, England, 1998).
 - ⁴⁹N. L. Peterson, *Phys. Rev.* **136**, A568 (1964).
 - ⁵⁰K. A. Gschneidner, in *Solid State Physics*, edited by F. Seitz and D. Turnbull (Academic Press, New York 1964), Vol. 16, p. 276.
 - ⁵¹M. Ondrejcek, W. Swiech, C. P. Flynn (unpublished).
 - ⁵²A. Latyshev, H. Minoda, Y. Tanishiro and K. Yagi, *Jpn. J. Appl. Phys., Part 1* **34**, 5768 (1995).
 - ⁵³Y. Cao and E. H. Conrad, *Phys. Rev. Lett.* **64**, 447 (1990).
 - ⁵⁴C. P. Flynn, *J. Phys. F: Met. Phys.* **18**, L195 (1988).
 - ⁵⁵C. P. Flynn, *Phys. Rev. B* **71**, 085422 (2005).
 - ⁵⁶C. P. Flynn (unpublished).